UCRL- 90357
PREPRINT

EQUATION OF STATE OF STRONGLY COUPLED PLASMA MIXTURES

H. E. DeWitt
University of California, Lawrence Livermore National Laboratory
Livermore, California 94550

This paper was presented at
Second International Conference/Workshop on
Radiative Properties of Hot Dense Matter
Sarasota, FL
October 31 - November 4, 1983

This paper was prepared for submittal to
Journal of Quantitative Spectroscopy

February 3, 1984

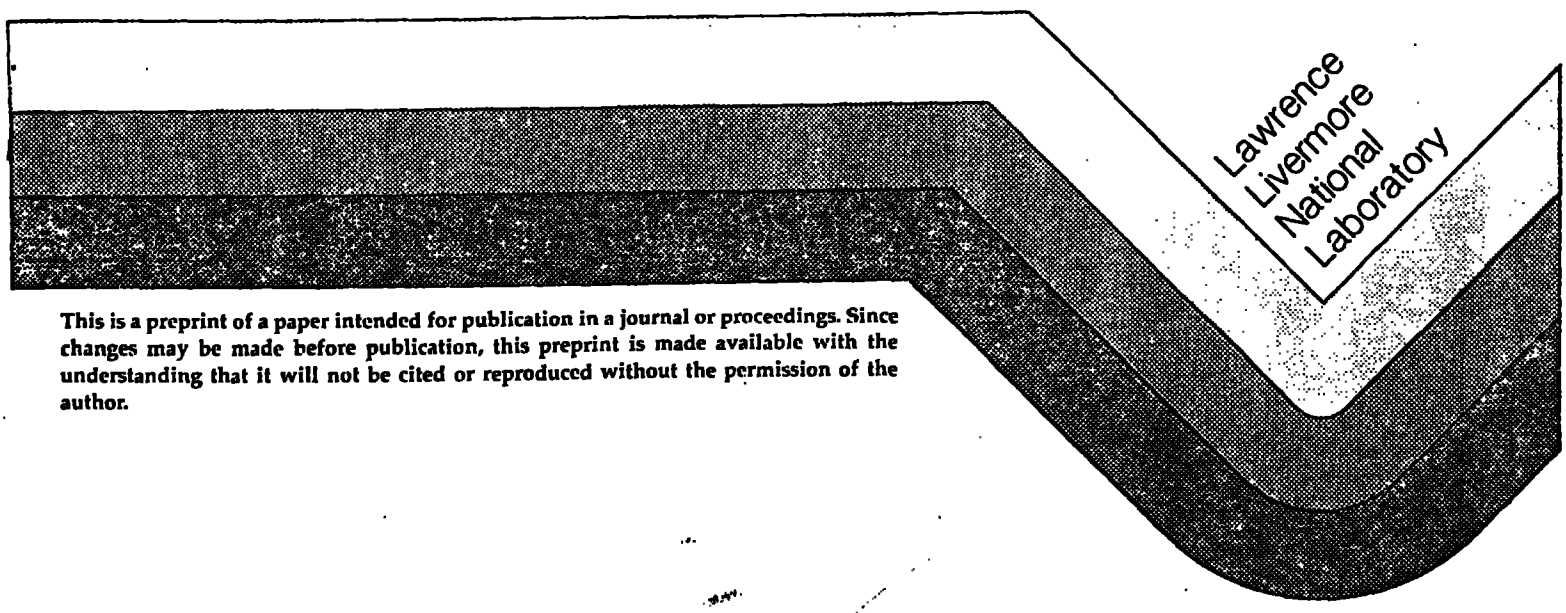

EQUATION OF STATE OF STRONGLY COUPLED PASMA MIXTURES*

Hugh E. DeWitt
University of California
Lawrence Livermore National Laboratory
Livermore, CA 94550

• Thermodynamic properties of strongly coupled (high density) plasmas of mixtures of light elements have been obtained by Monte Carlo simulations. For an assumed uniform charge background the equation of state of ionic mixtures is a simple extension of the one-component plasma EOS. More realistic electron screening effects are treated in linear response theory and with an appropriate electron dielectric function. Results have been obtained for the ionic pair distribution functions, and for the electric microfield distribution.

I. INTRODUCTION

The purpose of this paper is to give a short summary of current understanding of the thermodynamic properties of strongly coupled Coulombic systems and a few recent results. The state of matter described by the term 'strongly coupled plasma' is characterised as a partially or fully ionized system in which the thermodynamic properties are largely dominated by strong correlations induced by Coulomb interactions among the ions. Strongly coupled plasmas include the partially ionized plasmas in magneto-hydrodynamic generators, exploding wire experiments, laser-fusion compression experiments, liquid metals, interiors of large gaseous planets, many stellar interiors, white dwarf stars and neutron star crusts. For a more complete review of the large body of research in this area of physics during the past two decades the reader is referred to excellent review articles by Baus and Hansen[1] and by Ichimaru.[2]

---

*Work performed under the auspices of the U.S. Department of Energy by Lawrence Livermore National Laboratory under contract #W-7405-Eng-48.

The significant thermodynamic properties of these systems are largely determined by the Coulomb interactions among ions. The Coulomb potential will be modified by bound electron cores in the case of partially ionized plasmas and in general by the screening effect of the free electrons. Since the nuclear masses of the ions are large, the ion motion is, to a large extent, classical in most strongly-coupled plasmas. By contrast, the small mass of the electrons leads to the onset of Fermi degeneracy for the electrons at sufficiently high density so that the electron description is usually quantum mechanical. Since the electron Fermi energy is normally far larger than the average ion kinetic energy, kT, the electrons often become somewhat decoupled from the ions. The role of the electrons is to provide sufficently high pressure due to Fermi degeneracy to prevent the plasma from collapsing and to provide negative charge to neutralize the ions. Hence, a strongly coupled plasma may be regarded as a two-fluid mixture: a fluid of classical positive charges moving in the neutralizing electron fluid. The two fluids interact with each other mainly by means of the electron screening effect due to accumulation of fast moving electrons around each ion. Most of the computations of thermodynamic properties to date have made the additional approximation of regarding the electrons as a continuous fluid so that classical statistical-mechanical methods may be used for calculation of the ion-ion correlations. These methods use brute force numerical simulation of a few hundred ions by Monte Carlo or molecular dynamics procedures, or with appropriate integral equations from liquid state theory usually various forms of the hypernetted chain (HNC) equation.

Strongly coupled plasmas are mainly characterized by the classical Coulomb coupling parameter:

$$\Gamma = \frac{Z^{*2}e^2}{akT} \tag{1}$$

$$a = \left(\frac{4\pi}{3}\rho_i\right)^{-1/3}$$

where Z^* is nuclear charge in the case of bare nucleus or the effective ionic charge in the case of a partially ionized plasma. a is the ion sphere radius, and $\rho_i = N_i/V$ is the ion number density. The concept of Debye length is

not normally useful for description of a strongly coupled plasma. Electron screening for degenerate electrons requires a second parameter:

$$r_s = a_e/a_B \qquad (2)$$

$$a_e = \left(\frac{4\pi}{3}\rho_e\right)^{-1/3}$$

where a_e is the electron ion sphere radius (also called the Wigner-Seitz radius) and $\rho_e = Z^*\rho_i$. For ionic mixtures the parameter list will require the charge number of each ionic species and the chemical composition. For partially ionized plasmas additional parameters will be required for characterizing the bound electrons forming the ionic cores.

A summary of strongly coupled plasma properties for various possible systems could be given in terms of the following sequence of complexity:

1) Classical Point Ions in a Uniform Background (OCP). This system has been the subject of an enormous amount of numerical and analytical study. As a simple mathematical model it plays the same role in strongly coupled plasma physics as the hypothetical hard-sphere fluid plays in the theory of neutral liquids such as liquid argon. The OCP is approximated in nature in only extreme density astronomical objects, white dwarf stars and neutron stars.

2) Mixtures of Point Ions in a Uniform Background. This is essentially the OCP but with mixture of different nuclear charges. Simulations on this system give the means of testing simple mixing rules.

3) Point Ions in a Responding Background. In white dwarf stars the electron Fermi energy is relativistic and so large that the elecrons are well approximated by a uniform background. At lower densities as in liquid metals the electrons are degenerate but cluster around each ion in a manner that in some cases can be approximated by linear response theory and an appropriate electron dielectric function. This description applies, for example, to the interior of

the planet Jupiter for which the ionized hydrogen is a strongly coupled plasma with $\Gamma \sim 30$ and $r_s \sim 1$.

4) Partially Ionized Plasmas. Examples are found in magneto-hydrodynamic drivers, and laser-fusion experiments. The ion-ion potential now deviates signficantly from the Coulomb potential at short distances as the ion cores come into contact. Simple forms of the effective potentials for various ionization states that reproduce known ionic energy levels are available for use in numerical simulations and integral equations.[3] The effective ionic charge, $Z_i^* = Z_i - N_i$ where N_i is the number of bound electrons, must be obtained first with a suitable ionization equilibrium calculation.

The feature common to all the diverse systems described as strongly coupled plasmas is liquid-like behaviour in contrast to a gas-like description of weakly coupled plasmas. The strong correlations induced by the Coulomb interactions cause the short range order that shows up as oscillations in the ion-ion pair distribution function. At extreme densities as possibly in white dwarf stars and certainly for neturon star crusts the plasma goes into a crystalline state.

II. THE ONE-COMPONENT PLASMA (OCP)

Before discussing the mathematical abstraction called the OCP, it is useful to note that strongly coupled plasmas have a two-component Hamiltonian and that the total internal energy is given by a canonical ensemble average of that Hamiltonian:

$$\begin{aligned} E = \langle H \rangle &= \langle K_i + K_e + U_{ii} + U_{ei} + U_{ee} \rangle \\ &= \frac{3}{2} NkT + \frac{3}{5} N_e \epsilon_F + U \end{aligned} \tag{3}$$

where $N_e = ZN$, ϵ_F is the electron Fermi energy, and U is the average Coulombic interaction energy:

$$U/NkT = \frac{1}{NkT} \sum_{i>j}^{N} \frac{z_i z_j e^2}{|r_i - x_j|} - \sum_{i,\alpha}^{N_i N_e} \frac{z_i e^2}{|x_i - r_\beta|} + \sum_{\alpha<\beta}^{N_e} \frac{e^2}{|x_a - x_\beta|} \tag{4}$$

When the discrete electrons are replaced with a uniform background, U simplifies greatly to:

$$\begin{aligned} U/NkT &= \frac{1}{NkT} < \sum_{i<j}^{N} \frac{z_i z_j e^2}{|x_i - x_j|} + \text{background} > \\ &= \frac{1}{N} < \sum_{i<j}^{N} \frac{\Gamma}{|x_i - x_j|} + \ldots > \\ &= \frac{3}{2} \int_0^\infty x^2 dx \frac{\Gamma}{x} \left(g(x) - 1\right) \\ &= f(\Gamma) \\ x &= r/a \end{aligned} \tag{5}$$

where $f(\Gamma)$ indicates the function of the single parameter Γ which completely describes the thermodynamics of the system. In the weakly coupled or low density limit the energy fuction is given exactly by the Debye-Hückel result:

$$\begin{aligned} f(\Gamma) &= -\frac{1}{2} \cdot \frac{1}{4\pi\rho\lambda_D^3} \quad , \quad \Gamma << 1 \\ &= -\frac{\sqrt{3}}{2} \Gamma^{3/2} \end{aligned} \tag{6}$$

which is also the exact lower bound on the energy.[4] Deviations from the Debye results were first calculated using the cluster expansion for plasmas due to Abe.[5] Later it was found that the Abe expansion was embedded in the framework of the HNC equation which can now be used to give the function to adequate accuracy for $\Gamma < 1$.[6] At approximately $\Gamma \sim 1$, that is,

where the average Coulomb energy of an ion, z^2e^2/a, is approximately kT, the total Coulombic energy of the sytem may be divided into two parts:

$$U/NkT = \left(U_o(\rho) + U_{th}(\rho,T)\right)/NkT$$
$$= A\Gamma + g(\Gamma) \qquad (7)$$

where U_o is a static energy of the OCP fluid that is approximately the Madelung energy of a lattice of ions, and U_{th} is the thermal energy of the ions in this liquid-like system of charges with short range order. The constant A in Eq. 7 may be estimated from an elementary approach, the ion sphere model, which gives:

$$(U/NkT)_{\text{ion-sphere}} = -\frac{9}{10}\Gamma \qquad (8)$$

Equation 8 is also the exact Lieb-Narnhofer lower bound on the energy.[7] The Madelung constant for the lowest energy Coulomb lattice, the bcc lattice, is $A_{bcc} = -0.895929$, which is about .45% above the Lieb-Narnhofer lower bound. Presumably the bcc lattice is the true lowest possible energy of the OCP in the $\Gamma > \infty$ limit. Most simple theories of the OCP, e.g., the ion-sphere model, give $A = -9/10$ and the numerical solution of the HNC equation comes very close to this value.

Beginning with the pioneering work of Brush, Sahlin, and Teller[8] in 1966, the OCP has been studied in detail in the strongly coupled region, $\Gamma > 1$, by 'numerical experiments', numerical simulation by means of Monte Carlo or molecular dynamics. Readers should consult Refs. 1 and 2 for the earlier work. The most recent and most accurate Monte Carlo study was a joint Livermore and Los Alamos collaboration using Cray computers.[9,10] The total interaction energy function, $f(\Gamma)$, is shown schematically in Fig. 1 which indicates the OCP fluid and OCP solid phases. The actual change in the internal energy at the phase transition is quite small, only about .5% of the total enegy. The thermal energy of the two phases is shown on Fig. 2 with U_o defined to be the bcc lattice value. At the phase transition, which current data indicates at $\Gamma = 178$, the thermal energy is only 1.5% of the total energy so that extremely long and time-consuming Monte Carlo simulations

are required to give reasonable accuracy for the fluid state. In the recent study we used up to 1024 particles in the simulation and computed the average energy from as many as 40 million configurations. The total energies thus obtained are believed to be accurate to a few parts in 10^5. Hence, the thermal energies are believed to be known to about .1%. The question of accuracy is complicated by possible N dependence in the simulations, but empirically we found[10] that the number dependent correction was $O(\Gamma/N)$ and small enough to give a good result for the $N \to \infty$ limit.

An earlier analysis[11] of Monte Carlo simulation data for the OCP indicated that the thermal energy, U_{th}/NkT, behaved as a low power of Γ, probably $\Gamma^{1/4}$. DeWitt and Rosenfeld[12] using a variational hard-sphere model and the entropy obtained from the virial pressure of the Percus-Yevick equaton, found that OCP fluid energy could be expressed in an expansion of powers of $\Gamma^{1/4}$:

$$U/NkT = -\frac{9}{10}\Gamma + \left(\frac{8}{9}\right)^{1/4}\Gamma^{1/4} - \frac{1}{2} + \left(\frac{7}{80}\right)\left(\frac{18}{\Gamma}\right)^{1/4} + \ldots \qquad (9)$$

The most exact OCP Monte Carlo data obtained recently[10] is consistent with this analytic form. The fit to the data is:

$$U/N = -0.8977\,\Gamma + 0.9594\,\Gamma^{1/4} - 0.8149 + 0.1896\,\Gamma^{-1/4} + \ldots \qquad (10)$$

The pressure is obtained exactly for the OCP from the virial theorem as:

$$\beta P/\rho = \frac{1}{3}\beta U/N \qquad (11)$$

Equation 10 is the currently best available equation of state for the OCP. It is valid for the OCP fluid phase from approximately $\Gamma = .8$ to the freezing value of Γ at approximately 180. It also seems to fit well the small amount of Monte Carlo data so far obtained for the metastable OCP fluid for temperatures below the freezing temperature, i.e., for $\Gamma > 180$. For the OCP solid phase the energy was found to be that of the expected harmonic solid with a small anharmonic contribution:

$$\beta U/N = -0.895929\,\Gamma + \frac{3}{2} + 3225/\Gamma^2 + \ldots \tag{12}$$

The actual freezing value of Γ is difficult to locate precisely. The procedure used is to obtain the Helmholtz free enrgy for each phase using Eqs. 10 and 12. Thus, the Helmholtz free energy for the fluid phase is obtained by integrating Eq. 10:

$$\begin{aligned}\beta F/N &= \int_{\beta_1}^{\beta} \left(\beta U(\beta')/N\right) \frac{d\beta'}{\beta'} + \beta F(\beta_1)/N \\ &= \int_{\Gamma_1}^{\Gamma} \frac{d\Gamma'}{\Gamma'}\,\delta(\Gamma') + e(\Gamma_1)\end{aligned} \tag{13}$$

and the integration constant is obtained by numerical integration from $\Gamma = 0$ to $\Gamma_1 = 1$. A similar calculation of the Helmholtz free energy of th solid phase uses Eq. 12 and a lattice vibration constant for the bcc lattice (see Ref. 9). The location of the freezing transition is obtained from the crossing point of the fluid and solid free energies. Estimates of the freezing value of Γ obtained this way have ranged from $\Gamma \sim 125$ (Ref. 8) to $\Gamma = 178 \pm 1$ as our best current estimate.

The pure HNC equation was found in 1974 to be a moderately good representation of the OCP but gave an incorrect result for the thermal energy. Since the Monte Carlo simulations are very long and expensive, there has been considerable challenge to theorists to improve the HNC equation in such a manner as to reproduce as accurately as possible the Monte Carlo data. The relevant approxiamtions may be seen from the cluster diagrams for the pair distribution function and from the Ornstein-Zenicke equation:

$$\begin{aligned} g(r) &= \exp\left[-\beta u(r) + N(r) - B(r)\right] \\ h(r) &\equiv g(r) - 1 = c(r) + \rho\int d^3r'\, c(r')h\left(|\underset{\sim}{r} - \underset{\sim}{r}'|\right) \\ &= c(r) + N(r) \end{aligned} \tag{14}$$

$N(r)$ is the sum of all convolution diagrams, and $B(r)$ is the sum of the so-called bridge diagrams, i.e., those which have no convolutions. The HNC

equation is obtained with $B(r) = 0$. For the OCP, i.e., the Coulomb potential, $\beta u(r) = \Gamma/x$. Ng[6] solved the equation with an interactive method to great accuracy for $g(r)$, and the interaction energy was obtained to eight figure accuracy from Eq. 5. A comparison of the Monte Carlo results for $g(r)$ with the HNC $g(r)$ suggested an appropriate form for the bridge graph function. Rosenfeld and Ashcroft showed that the bridge function for the OCP and other simple solids could be well approximated by a hard sphere form obtained from the analytic solution of the Percus-Yevick equation.[13] The appropriate value of the effective hard sphere required for the bridge function is obtained by imposing the requirement of thermodynamic consistency. We have recently solved this modified HNC equation, and found that the $g(r)$ results in the energy integral agree with the Monte Carlo OCP energies to five figures for all values of Γ in the fluid phase.[14] Figure 3 shows the comparison of the modified HNC $g(r)$ solution with the Monte Carlo $g(r)$ for $\Gamma = 170$. There is slight deviation from the MC data near the first peak and the first valley which indicates that the hard sphere bridge graph is slightly incorrect. Nevertheless, the modified HNC equation is sufficiently accurate that it can be used for practical calculations of thermodynamic quantities for other strongly coupled plasmas in a small fraction of the time required for the Monte Carlo simulations.

III. EQUATION OF STATE OF BINARY IONIC MIXTURES

The discussion in this section may be applied to any number of different point nuclear charges in a responding electron background, but for simplicity we consider here two nuclear components of charge Z_1 and Z_2 with chemical compositions:

$$x_1 = N_1/(N_1 + N_2) \ , \ x_2 = N_2/N_1 + N_2)$$

The Helmholtz free energy for the mixture may be expressed as a function of a number of parameters in the following manner:

$$F_I/NkT = f_2 \ (Z_1, X_1, Z_2, X_2, \Gamma_o, r_s) \qquad (15)$$

where f_m denotes the free energy function for m ionic components and

$$\Gamma_o = e^2/akT \tag{16}$$

The problem is to find a simple mixing rule which as far as possible requires only a knowledge of f_1, the free energy function for the OCP. This is possible in the absence of electron screening, i.e., when $r_s = 0$. We first note that given a free energy function as state in Eq. 15 that the energy is obtained from a temperature derivative:

$$U/NkT = \Gamma_o \frac{\partial f_m}{\partial \Gamma_o} \tag{17}$$

and the pressure is obtained by differentiation with respect to volume:

$$PV/NkT = \frac{1}{3}\left\{\Gamma_o \frac{\partial f_m}{\partial \Gamma_o} - r_s \frac{\partial f}{\partial r_s}\right\} \tag{18}$$

In the absence of electron screening, Eq. 18 reduces to th virial theorem result.

A large amount of numerical simulation data is available from Monte Carlo runs done at Livermore and Los Alamos for binary ionic mixtures both with and without electron screening. Hansen and his colleagues in Paris have also reported extensive results on mixtures.[15] We first note that the ion sphere model gives an elementary extension of the OCP reseult, Eq. 8:

$$(U/NkT)_{mixture} = -\frac{9}{10}\,\overline{z^{5/3}}\,\bar{z}^{1/3}\,\Gamma_o \tag{19}$$

where

$$\overline{z^s} = z_1^{\,s} x_1 + z_2^{\,s} x_2 \tag{20}$$

Our simulations in strong coupling ($\Gamma_o >> 1$) for a wide variety of mixtures and of charge numbers as far apart as $Z_1 = 1$ and $Z_2 = 10$ amply

confirmed the correctness of the ion sphere mixing rule for the binary mixture fluid static energy, the generalization of U_o in Eq. 7. As in the OCP case, the mixture thermal energy is less certain. Hansen, et al.[5] suggested the 'linear law' as a suitable fit to their Monte Carlo and HNC mixture data:

$$F_I/NkT = x_1 f_1(z_1^{5/3}\,\bar{z}^{1/3}\,\Gamma_o) + x_2 f_1(z_2^{5/3}\bar{z}^{1/3}\,\Gamma_o) \tag{21}$$

where f_1 is the OCP free energy function as obtaned from EQ. 13 (see Ref. 11). The same mixing rule clearly applies to the internal energy and the pressure using Eqs. 10 and 11. This mixing rule fairly well predicts the Monte Carlo mixture results that have been generated to date for

$$\bar{z}^{5/3}\,\bar{z}^{1/3}\,\Gamma_o > 1 \quad ,$$

as might be expected since this rule reproduces the ion--sphere model result. It is clear, however, that Eq. 21 cannot be a completely general result for mixtures of all degree of coupling since it is incorrect in the weak coupling limit for which the Debye-Huckel result is:

$$F_I/NkT = -\frac{\sqrt{3}}{3}\,(\bar{z^2})^{3/2}\,\Gamma_o^{3/2} \tag{22}$$

Using arguments based on the known lower bounds for the free energy, i.e., the Debye results for weak coupling and the Lieb-Narnhofer results for strong coupling, Rosenfeld has obtained mixing rule which satisfies both limits:[16]

$$F_I/NkT = \frac{\bar{z}}{\bar{z^2}}\left\{x_1 z_1 f_1\left(\frac{z_1^{2/3}\,\bar{z^2}\,\bar{z}^{1/3}}{\bar{z}}\,\Gamma_o\right)\right. \tag{23}$$

$$\left. + x_2 z_2 f_1\left(\frac{z_2^{2/3}\,\bar{z^2}\,\bar{z}^{1/3}}{\bar{z}}\right)\right\}$$

In strong coupling the Rosenfeld mixing rule, Eq. 23, satisfies our available Monte Carlo mixture data slightly less well than the linear law, Eq. 21. However, the inherent errors in the Monte Carlo data due to limited length of the simulations and the number dependence does not make it possible as yet to definitely decide whether Eq. 21 is to be preferred over Eq. 23. In the intermediate coupling regime, $\Gamma_o < 1$, Eq. 23 is probably more accurate since it tends to the correct limiting result in weak coupling. For calculations of the screening enhancement of the thermonuclear reaction rates in stellar interiors[17] the Rosenfeld mixing rule is probably more appropriate than the linear law.

For the situation with a responding background of electtrons the mixture probem is made more complicated by the r_s dependence. The approach taken to analyze the Monte Carlo simulations in which the electron background is treated as a polarizable fluid described by linear response theory has been to assume a model free energy of the form:

$$F_I/NkT = A\Gamma_o + B\Gamma_o^{1/4} + C\ell n\Gamma_o + D \qquad (24)$$

(Existing data does not justify the inclusion of a $\Gamma^{-1/4}$ term at this time.) For the OCP, Eq. 24 would simply be the function f_1 from Eq. 13. In general the coefficients A,B,C, and D are treated as functions of the charge numbers, the chemical compositions, an r_s. In linear response theory it is easily demonstrated that the screening correcton to the OCP and the binary mixture results in a uniform background, Eq. 21 or 23, begins with a linear term in r_s. Initial results for screening corrections to the ionized hydrogen in Jupiter and for fully ionized hydrogen-helium mixtures were given for a large number of simulations from Lvermore in 1976.[18] The Lindhard dielectric function was used for the description of electron screening. Our more recent Monte Carlo mixture simulations on hydrogen and helium mixtures used longer runs and values of r_s up to about 1.5.[19] We found that at least for the mixture static energy term, i.e., the coefficient A, that a quadratic dependence on r_s was present. The coefficients of powers of Γ_o in Eq. 24 were written as:

$$A = a_1[X_1 z_1^{5/3} + X_2 z_2^{5/3}] + r_s[a_2 X_1 + a_3 X_2] + r_s^2\,[a_2 X_1 + a_2 X_2] \qquad (25)$$

$$B = b_1[X_1 z_1^{5/12} + X_2 z_2^{5/12}] + r_s[b_2 X_1 + b_3 X_2] \qquad (26)$$

$$C = c_1 + r_s\,[X_1 c_2 + X_2 c_3] \qquad (27)$$

$$D = d_1 - c_1 X_2\, \ell n(z_2/z_1)^{5/3} + r_s[d_3 X_1 + d_4 X_2] \qquad (28)$$

The unscreened coefficients in Eqs. 25 to 28 were taken from a fit to OCP data, and the powers of z_1 and z_2 are those obtained from the ion-sphere model and the linear law, Eq. 21. With these first four coefficients determined, we still had 10 remaining coefficients to fit to our Monte Carlo mixture energy and pressure data. This was done with a least-squares procedure. For each run we calculated the model value of the interaction energy and the pressure (from Eqs. 17 and 18), and then computed the residuals between the model values and the Monte Carlo values. The residuals were squared, summed, and the 10 parameters were adjusted until the sum was minimized. The results are shown in Table I.

TABLE I. Values of coefficients in the model interaction free energy, Eq. 24.

$ad_1 = 0.89461$	$a_2 = 0.04663$	$a_3 = 0.46312$
	$a_4 = -0.00479$	$a_5 = -0.04909$
$b_1 = 3.26591$	$b_2 = -1.7441$	$b_3 = 2.71013$
$c_1 = -0.50123$	$c_2 = -0.17267$	$c_3 = 1.47087$
$d_1 = -2.81630$	$d_3 = 1.13216$	$d_4 = -2.31857$

The r_s dependence in this free energy model is more general than the 1976 model because of the presence of te r_s^2 terms in $A(r_s)$. This is essential to properly fit the Monte Carlo data for the pressure. Note that a_4 and a_5 are small compared with a_2 and a_3, the coefficients for the term linear in r_s. The primary effect of the electron screening is to

increase the magnitude of $A(r_s)$. Since $A(r_s)$ is negative as a consequence of the electron background, the 'static' energy of the dense plasmas is lowered significantly for $r_s \sim 1$. The physical reason for this lowered fluid energy is the increased density of free electrons clustered around each ionic nucleus. The pressure change due to screening is very small since the pressure is little affected by the screening cloud of electrons surrounding each ion. Indeed, since $r_s \Gamma_o$ in the free energy model is independent of density, it is apparent that this term will give no contribution to the pressure. Consequently the actual change of pressure due to electron screening is largely determined by the r_s^2 terms. This pressure change is small and positive.

IV. ELECTRIC MICROFIELD IN STRONGLY COUPLED PLASMAS

The Monte Carlo code used to simulate the energy and pressure of strongly coupled plasmas can also generate the electric microfield distribution around a given ion due to neighboring ions. Such microfields are needed for the calculation of spectral line shapes due to the Stark effect for high Z temperature laser-induced plasmas. For temperatures in the hundreds of eV range, highly stripped neon and argon plasmas can be fproduced in which the eelectrons are non-degenerate. The ion-ion potential in this situtation can be described with a screened Coulomb form and a Debye length due to electrons:

$$U_{ii}(r) = \frac{(ze)^2}{r} e^{-r/\lambda_{De}}, \quad \lambda_{De} = \left(\frac{kT}{4\pi e^2 n_e}\right)^{1/2}$$

n_e is the electron number density and Z is the effective charge of the partially stripped ion. To compute the electric microfield for plasmas in these conditons the Monte Carlo code was modified slightly by inserting the high temperature Debye electron dielectric function:

$$\epsilon(k) = 1 + 1/(k\lambda_{De})^2 \tag{30}$$

Monte Carlo runs with 50 charges an 200,000 configurations were sufficient to give accurate microfield sitrbutions along with the usual U/NkT, PV/NkT and g(r) results.

Detailed comparisons of the MOnte Carlo microfields with recent microfield theories are given in a recent report.[20] Figure 4 shows the Monte Carlo microfield for hydrogenic neon with $\Gamma = 4.32$. The detailed many-body treatment of Tighe and Hooper[21] and also the simpler Independent Perturber (IP) Model compare favorably with th Monte Carlo microfield which may be regarded as a 'numerical experimental result'. This kind of comparison indicates that the numerical simulation of microfields plays a very useful role in providing a guide for developing better theoretical calculations of microfield distributions for future experiments.

HED:mpd:0678A

REFERENCES

1. M. Baus and J. P. Hansen, Physics Reports 59, 1 (1980).

2. S. Ichimaru, Rev. Mod. Phys. 54, 1017 (1982).

3. F. J. Rogers, Phys. Rev. A23, 1008 (1981).

4. N. D. Mermin, Phys. Rev. 137, 1441 (1965).

5. R. Abe, Prog. Theo. Phys. 22, 213 (1959).

6. K. C. Ng, J. Chem. Phys. 61, 2680 (1974).

7. E. H. Lieb and N. Narnhofer, J. STAT. Phys. 14, 465 (1976).

8. S. G. Brush, H. L. Sahlin, and E. Teller, J. Chem. Phys. 45, 21 2 (1966).

9. W. L. Slattery, G. D. Doolen, an H. E. DeWitt, Phys. Rev. A21, 2087 (1980).

10. W. L. Slattery, G. D. Doolen, and H. E. DeWitt, Phys. Rev. A26, 2255 (1982).

11. H. E. DeWitt, Phys. Rev. A14, 1290 (1976).

12. H.E. DeWitt and Y. Rosenfeld, Phys. Rev. Lett 75A, 79 (1979).

13. Y. Rosenfeld and N. W. Ashcroft, Phys. Rev. A20, 1208 (1979).

14. F. J. Rogers, d. A. Young, H. E. DeWiot, and M. Ross, Phys. Rev. A28, 2290 (1983).

15. J. P. Hansen, G. M. Torrie, P. Viellefosse, Phys. Rev. A16, 2153 (1977).

16. Y. Rosenfeld, Phys. Rev. A26, 3622 (1982).

17. N. Itoh, H. Totsuji,S. Ichimaru, and H. E. DeWitt, Astrophys. J. 234, 1079 (1979).

18. H. E. DeWitt andW. B. Hubbard, Astrophys. J. 205, 295 (1976).

19. W. B. Hubbard and H. E. DeWitt, sumbitted to Astrophys. J. A preliminary report of this work may be found in a Lvermore report, UCID-18574-82-2 (1982).

20. C. A. Iglesias, C. F. Hooper, Jr. and H. E. DeWitt, Phys. Rev. A28, 361 (1983).

21. R. J. Tighe and C. F. Hooper, Jr., Phys. Rev. A15, 1773 (1977).

Figure Captions

FIG. 1 Schematic representation of the OCP Coulombic interaction erngy for the fludid and solid phases. The two curves are nearly straight lines because of th dominance of the static energy.

FIG. 2 Thermal energy for both the fluid and solid OCP phases. The error bars are hardly visible at this scale.

FIG. 3 $g(r)$ for the OCP fluid at $\Gamma = 170$. Solid line is the solution of the modified HNC equation, and x's are representative Monte Carlo values.

FIG. 4 A comparison of the microfield distributions calculated with IP and TH methods with Monte Carlo results (MC). All ionic consistuents carry a charge of +9. The dimensionless field variable is scaled in terms of the electron sphere radius.

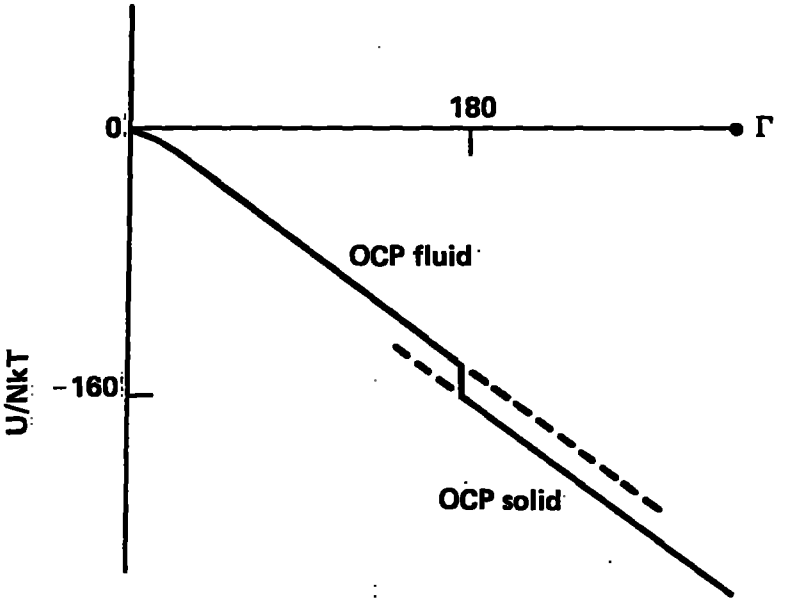
0
180
Γ
OCP fluid
U/NkT
-160
OCP solid

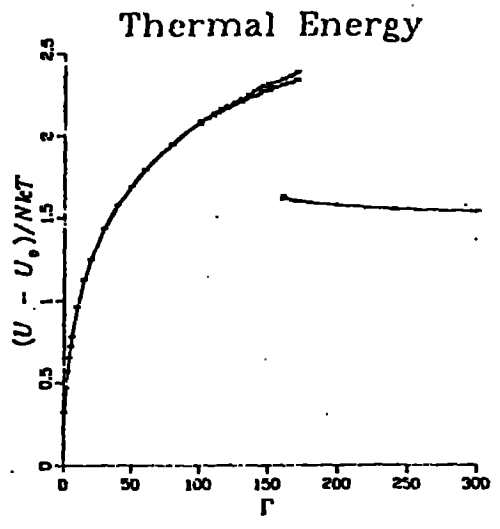
Thermal Energy
$(U - U_0)/NkT$
0
0.5
1
1.5
2
2.5
0
50
100
150
200
250
300
Γ

Fig. 3

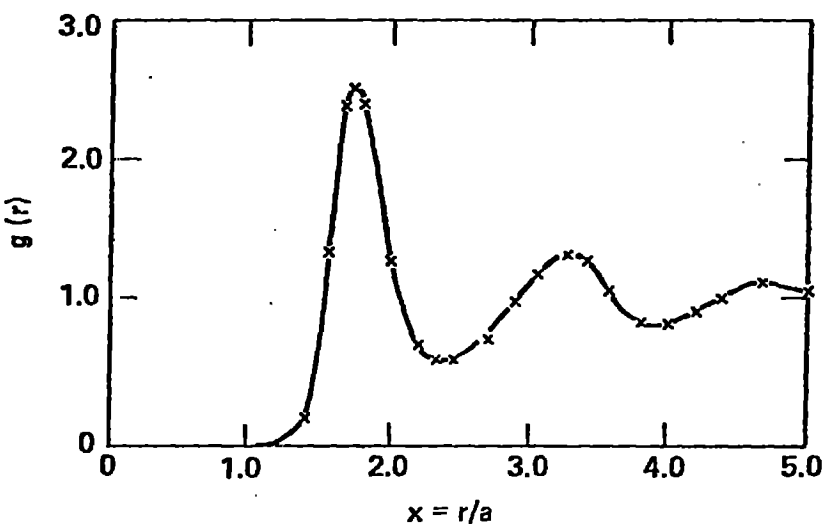

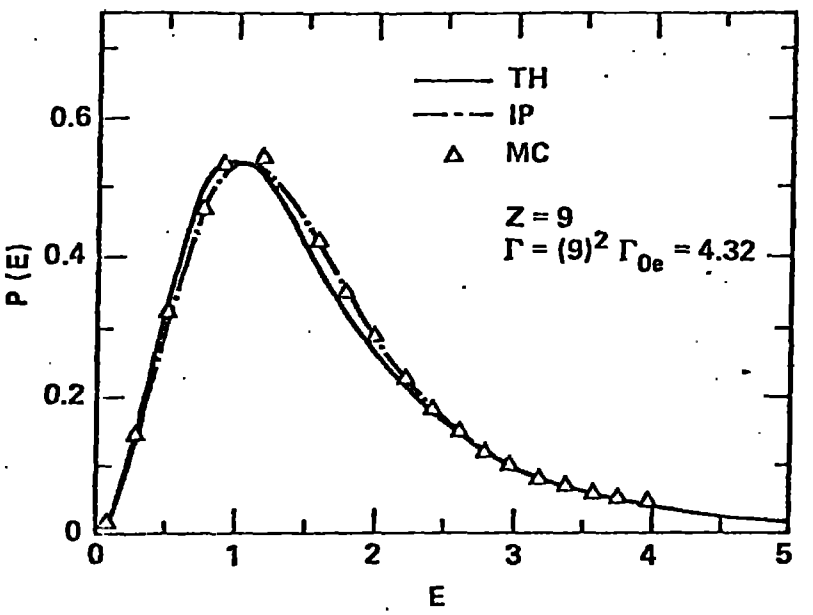
TH
IP
MC
Z = 9
Γ = (9)² Γ0e = 4.32
P (E)
E
0
0.2
0.4
0.6
0
1
2
3
4
5